*6998–7008* *Nucleic Acids Research, 2011, Vol. 39, No. 16* *Published online 19 May 2011*
*doi:10.1093/nar/gkr371*

# Phosphorylation of Mcm2 modulates Mcm2–7 activity and affects the cell's response to DNA damage

**Brent E. Stead, Christopher J. Brandl and Megan J. Davey***

Department of Biochemistry, Schulich School of Medicine & Dentistry, University of Western Ontario, London, ON, Canada, N6A 5C1

Received November 16, 2010; Revised April 27, 2011; Accepted April 28, 2011

## ABSTRACT

**The S-phase kinase, DDK controls DNA replication through phosphorylation of the replicative helicase, Mcm2–7. We show that phosphorylation of Mcm2 at S164 and S170 is not essential for viability. However, the relevance of Mcm2 phosphorylation is demonstrated by the sensitivity of a strain containing alanine at these positions (*mcm2$_{AA}$*) to methyl methanesulfonate (MMS) and caffeine. Consistent with a role for Mcm2 phosphorylation in response to DNA damage, the *mcm2$_{AA}$* strain accumulates more RPA foci than wild type. An allele with the phosphomimetic mutations S164E and S170E (*mcm2$_{EE}$*) suppresses the MMS and caffeine sensitivity caused by deficiencies in DDK function. *In vitro*, phosphorylation of Mcm2 or Mcm2$_{EE}$ reduces the helicase activity of Mcm2–7 while increasing DNA binding. The reduced helicase activity likely results from the increased DNA binding since relaxing DNA binding with salt restores helicase activity. The finding that the ATP site mutant *mcm2$_{K549R}$* has higher DNA binding and less ATPase than *mcm2$_{EE}$*, but like *mcm2$_{AA}$* results in drug sensitivity, supports a model whereby a specific range of Mcm2–7 activity is required in response to MMS and caffeine. We propose that phosphorylation of Mcm2 fine-tunes the activity of Mcm2–7, which in turn modulates DNA replication in response to DNA damage.**

## INTRODUCTION

DNA replication is a tightly regulated process that occurs once and only once per cell division cycle. In addition, the cell must respond to impediments to replication, including DNA damage. One of the targets for regulation is the replicative helicase, comprised of minichromosome maintenance proteins 2 through 7 (Mcm2–7). Unlike other replicative helicases, which contain six identical subunits, Mcm2–7 is comprised of six distinct, but related subunits (1). The requirement for six subunits, with distinct sequences is thought to reflect individual roles for each subunit. Notably, the contribution of subunits to adenosine triphosphate (ATP) hydrolysis by the intact complex varies widely (2–4). For example, mutations that severely affect ATP hydrolysis by Mcm2 do not strongly affect DNA unwinding by Mcm2–7 or viability of *Saccharomyces cerevisiae* (5,6). We have proposed that ATP hydrolysis by Mcm2 regulates DNA binding by Mcm2–7 since mutations that decrease ATP hydrolysis by Mcm2 increase binding to single-stranded DNA (6).

Mcm2–7 is targeted by several different kinases including CK2, cyclin-dependent kinases (CDK) and Mec1 (7–12). Importantly, Mcm2–7 is the principal target of the essential S-phase kinase, DDK (12,13). DDK, which is comprised of Dbf4 and Cdc7 subunits, activates DNA unwinding by Mcm2–7 *in vivo*, thereby triggering origin firing throughout S phase (12,14,15). Several of the Mcm subunits are phosphorylated by DDK, including Mcm2 (11,13,16–26). Multiple roles for the phosphorylation of Mcm2 by DDK have been postulated (21,22,24,25). Here, we examined the effects of DDK phosphorylation of Mcm2 on the activity and function of Mcm2–7 *in vitro* and *in vivo*. Our results suggest that DDK phosphorylation of Mcm2 is not required for viability, but is important for the cell's response to DNA damage, possibly through regulating DNA binding and/or DNA unwinding by Mcm2–7.

## MATERIALS AND METHODS

### Materials

Caffeine, hydroxyurea, methyl methanesulfonate (MMS), calcafluor white and ATP were from Sigma Aldrich

*To whom correspondence should be addressed. Tel: +(519) 661 2111 ext. 81414; Fax +(519) 661 3175; Email: mdavey5@uwo.ca

(≥99 % purity), molecular biology enzymes from New England BioLabs and primers from Integrated DNA Technologies.

## Plasmids

All DNA was amplified with Elongase polymerase (Invitrogen) and the primers mentioned in Supplementary Table S1. Plasmids are described in Supplementary Table S2. Mutated *mcm2* fragments were generated using megaprimer polymerase chain reaction (PCR) (27) and inserted into the NdeI/BamHI sites of pET16b, pET24a and/or pMD240. pMD423 and pMD422 were generated by inserting the BsrGI–BamHI fragment of pET24a-$mcm2_{K549R}$ into the same sites of pMD388 and pMD328, respectively. For pMD367 and pMD371, SphI–BamHI fragments from pET16b-$mcm2_{AA}$ and pET16b-$mcm2_{EE}$ were inserted into YCplac211 (28). pMD408 is YCplac211 with the XbaI–BamHI fragment of pET16b-*MCM2*. pMD397 is the BglII–StuI fragment of pET16b-*bob1* (a gift from M. O'Donnell, Rockefeller University) in YCplac211. pMD295 and pMD281 are *CDC7* and *DBF4* inserted into the NdeI/BamHI sites of pCDF-Duet (Novagen) and pET16b (Novagen), respectively. pMD449 contains *RFA1,* amplified from the yeast genome, fused in-frame to green fluorescent protein (GFP) in YCpDed-GFP (29) using NotI and SacI (blunted).

### Yeast strains

Two-step gene replacement (30) was employed to insert *mcm2* alleles into BY4743 (*MATa/α his3Δ1/his3Δ1 leu2Δ0/leu2Δ0 ura3Δ0/ura3Δ0 MET15/met15Δ0 LYS2/lys2Δ0*; (31)). Briefly, pMD367 ($mcm2_{AA}$) or pMD371 ($mcm2_{EE}$) digested with BsrGI or PstI, respectively, was transformed into BY4743, then Ura+ transformants were streaked on media containing 5-FOA. Colonies from 5-FOA were screened by sequencing, generating MDY104 (*MCM2*/$mcm2_{AA}$) and MDY106 (*MCM2*/$mcm2_{EE}$). MDY139 and MDY159 are spore colonies derived from MDY104 or MDY106 containing $mcm2_{AA}$ or $mcm2_{EE}$, respectively. The *URA3* gene was integrated downstream of *mcm2* by transforming YCplac211 containing *MCM2* (nucleotides 2023–2607; pMD408) digested with MscI into MDY139 and MDY159 to generate MDY169 and MDY191, respectively. A Ura+ strain wild type for *MCM2* (BY4741) was similarly generated (MDY167). Two-step gene replacement was used to generate a *cdc7Δ bob1* strain. BY23713 [*MATa/α ura3Δ0/ura3Δ0 leu2Δ0/leu2Δ0 his3Δ1/his3Δ1 lys2Δ0/LYS2 met15Δ0/MET15 can1Δ::LEU2+-MFA1pr-HIS3/CAN1 CDC7/cdc7::kanMX*; (32)] was transformed with YCplac211-*bob1* linearized with MscI. A *MATa cdc7Δ bob1* haploid (MDY210) was generated using 'Magic Marker' technology (32) and resistance to G418.

### Proteins

Mcm2–7 containing PKA-tagged Mcm3 was reconstituted from purified subunits as previously described (3,6). Purified proteins and complexes are shown in Supplementary Figure S1. DDK was purified from cells co-expressing Cdc7 (pMD295) and 6xHis-tagged Dbf4 (pMD281). Lysates, prepared as described (3), were applied to a 20 ml Ni–Sepharose column equilibrated in buffer C (20 mM Tris–HCl pH7.9, 500 mM NaCl, 10% glycerol) with 5 mM imidazole and washed with the same buffer followed by buffer C with 30 mM imidazole. Bound proteins were eluted with a 200 ml, 30 mM–1 M imidazole gradient in buffer C. DDK-containing fractions were dialyzed against 20 mM Tris–HCl pH 7.5, 0.1 mM ethylenediaminetetraacetic acid (EDTA), 10% glycerol and 50 mM NaCl. After dialysis, DTT was added to a final concentration of 2 mM and the dialysate applied to a 1-ml Mono Q column equilibrated in buffer A (20 mM Tris–HCl pH 7.5, 0.1 mM EDTA, 2 mM DTT and 10% glycerol) containing 50 mM NaCl. After washing with the same buffer, retained proteins were eluted with 50–500 mM NaCl in buffer A. Dbf4 and Cdc7 in peak fractions were verified by western blotting with anti-Dbf4 and anti-Cdc7 antibodies (Santa Cruz Biotechnology) and matrix-assisted laser desorption/ionization (MALDI) mass spectrometry (London Regional Functional Proteomics Facility).

### Fluorescence-activated cell sorting

Cells ($7 \times 10^6$), fixed in 70% ethanol, were prepared for fluorescence-activated cell sorting (FACS) by incubation with 200 μg RNase A per milliliter for 3 h at 37°C followed by 2 mg Proteinase K per milliliter for 30 min at 30°C. After staining with Sytox Green (Invitrogen), cell sorting was performed on a FACSCalibur (BD Biosciences) by the London Regional Flow Cytometry Facility.

### ATP hydrolysis and DNA unwinding assays

ATPase and helicase assays were performed as described (6), except that for DNA unwinding PEG 3350 was added to 5%. For reactions containing DDK, the indicated amounts of DDK were incubated with 200 nM Mcm2–7 and 5 mM ATP for 30 min at 30°C with 50 mM creatine phosphate and 2 μg/ml creatine phosphokinase and started by addition of oligonucleotide substrate. Statistical analyses were performed using analysis of variance (ANOVA) with Tukey's Multiple Comparison test.

### DNA binding

The gel filtration-based assay has been described previously (6). For DNA binding by electrophoretic mobility shift assays (EMSAs), 1 nM of 5′-end $^{32}$P-labeled poly-d($T_{60}$) was incubated with Mcm2–7 complex for 10 min at 37°C in 6 μl of reaction buffer. Glycerol was added to a final concentration of 5% (v/v) and the reaction then applied to a 5% native (Tris–borate–EDTA) polyacrylamide gel (19:1 acrylamide:Bis–acrylamide; BioShop Canada) containing 5% glycerol, 0.1% NP-40 and 10 mM $Mg(CH_3COO)_2$. The gel was resolved at 30 mA for 3 h, dried and exposed to a PhosphorStorage screen and imaged on a Storm 860 scanner (GE Healthcare).

## RESULTS

### Serines 164 and 170 of Mcm2 are not essential for normal growth

We mapped DDK's target sites in *S. cerevisiae* Mcm2 to serines 164 and 170 using *in vitro* kinase assays on N-terminal deletions and point mutations of Mcm2 (Supplementary Figure S2A–D). S164 and S170 were identified as DDK sites by another group while this study was ongoing (21). We tested whether loss of the potential DDK phosphorylation sites in Mcm2 affected growth using plasmid shuffling. The strain MDY054, containing wild-type MCM2 on a *URA3*-plasmid, was transformed with a *LEU2* plasmid encoding $mcm2_{S164A}$, $mcm2_{S170A}$, $mcm2_{S164A,S170A}$ ($mcm2_{AA}$) or wild-type *MCM2* under control of the *MCM6* promoter. The resulting strains were plated on 5-FOA, which is metabolized to a toxic product by Ura3, thus testing whether the *mcm2* allele encoded on the *LEU2*-containing plasmid supports viability. All of the alleles including $mcm2_{AA}$ supported viability with growth being comparable to that of cells with wild-type *MCM2* at 30°C and 37°C (Figure 1A). A slight reduction in growth was observed with $mcm2_{AA}$ at 16°C, whereas strains with the single mutations grew comparably to strains with wild-type *MCM2* (Figure 1A). Similar results were observed when $mcm2_{AA}$ was integrated at the *MCM2* locus (data not shown). We concluded that S164 and S170 are not essential for yeast viability under normal growth conditions. To further test the effects of mutating S164 and S170 on cell growth, we compared *MCM2* and $mcm2_{AA}$ strains by FACS. Comparison of asynchronously growing cultures indicated the same ratio of cells with 1C and 2C DNA content (Figure 1B). As shown in Figure 1C, the strains also had similar profiles after arrest in G1 with α factor mating pheromone followed by release. Together, these results indicate that there are no gross abnormalities in S phase nor DNA replication initiation when S164 and S170 are substituted with Ala.

In addition to its essential role in the initiation of DNA replication, DDK participates in the S-phase checkpoint response (12,33–39). Notably, mutations in *S. cerevisiae* or *Schizosaccharomyces pombe* Dbf4/Dfp1 result in sensitivity to drugs that induce the S-phase checkpoint, such as hydroxyurea (HU) and MMS (37,38,40,41). To determine whether phosphorylation of Mcm2 by DDK plays a role in the checkpoint response, we subjected cells supported for growth by a plasmid-encoded copy of *mcm2* to HU or MMS. Strains containing $mcm2_{AA}$ are more sensitive than wild-type *MCM2* strains to a short-term exposure of MMS but not HU (Figure 2A). When the strain containing $mcm2_{AA}$ was grown on YPD containing caffeine, its growth was also reduced (Figure 2B). Caffeine is a purine analog that inhibits phosphatidylinositol 3 kinase (PI3K)-like kinases, including those involved in the S-phase checkpoint (Tel1 and Mec1) and cell growth [TOR; (42–45)]. The doses of caffeine used here likely cause DNA damage (42). The sensitivity to caffeine was only observed with alanine mutations at both S164 and S170 ($mcm2_{AA}$); single mutations did not affect growth (Figure 2B), suggesting that, at least with respect to caffeine sensitivity, S164 and S170 are functionally redundant. Caffeine also affects the cell wall integrity pathway (46); however, the $mcm2_{AA}$ strain was not sensitive to calcofluor white (Figure 2C) indicating that phosphorylation at S164 and S170 is not required for the cell wall integrity pathway.

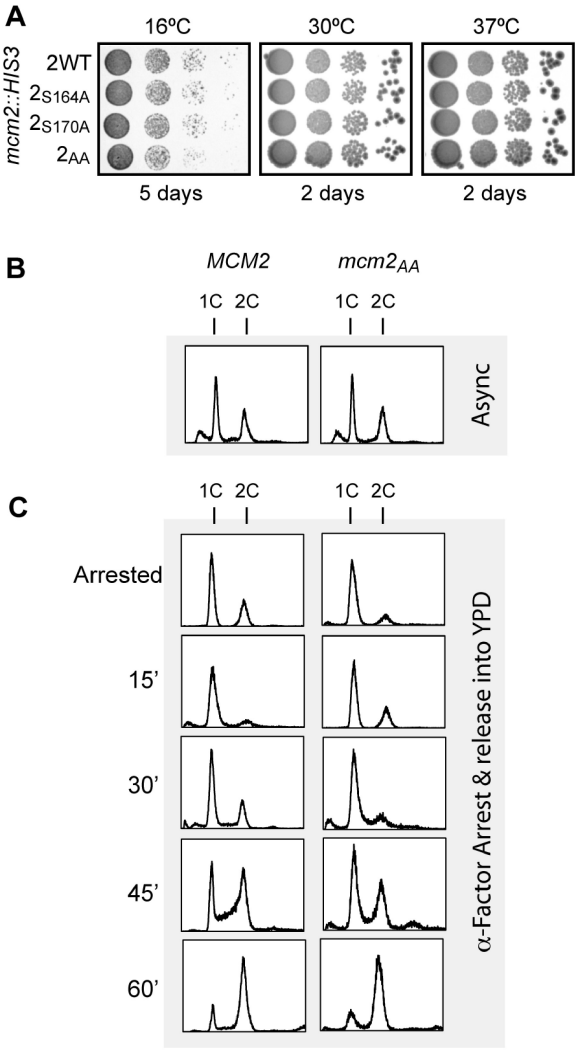


**Figure 1.** Strains containing mutations in the Mcm2 phosphorylation sites are viable. (**A**) The growth of haploid *mcm2Δ* strains bearing plasmid-encoded *MCM2* (WT), $mcm2_{S164A}$, $mcm2_{S170A}$ or $mcm2_{AA}$ was compared. Serial 10-fold dilutions of the strains were spotted on YPD plates and grown at the indicated temperatures. (**B**) FACS of *MCM2* and $mcm2_{AA}$ strains was performed on asynchronously growing cultures. (**C**) *MCM2* and $mcm2_{AA}$ cells were treated with α-factor mating pheromone for 3 h at 30°C, washed and resuspended in YPD. The DNA content of an aliquot of fixed cells was analyzed by FACS while arrested and at the indicated times after release.

### Phosphomimetic mutations at S164 and S170

We asked whether substitution of glutamic acid for serine at positions 164 and/or 170 provided a phosphomimetic effect by examining the drug sensitivity of cells bearing these mutations. Strains with the single ($mcm2_{S164E}$, $mcm2_{S170E}$) or the double mutant ($mcm2_{EE}$) alleles on

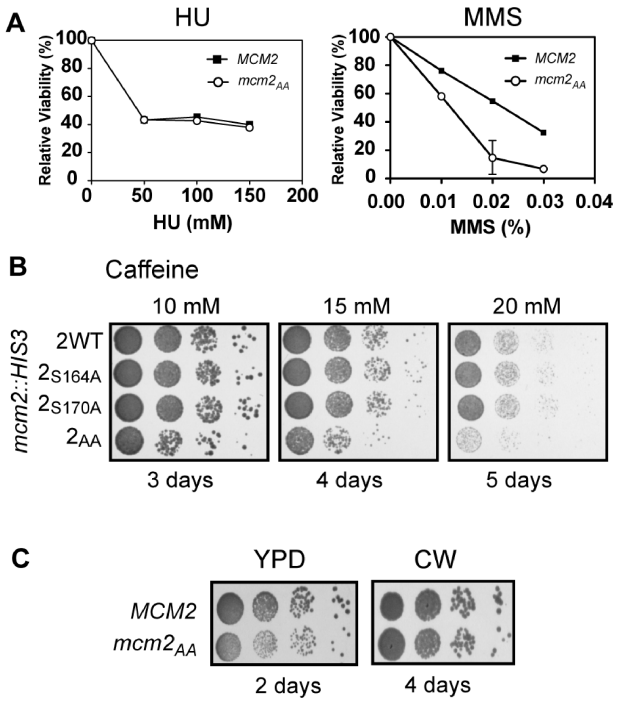


**Figure 2.** Sensitivity of $mcm2_{AA}$ to genotoxic agents. (**A**) The survival of *MCM2* and $mcm2_{AA}$ strains after a 4-h exposure to the indicated concentration of HU or MMS relative to untreated cells was measured as described (37). The assay was performed in triplicate and plotted as mean percent survival ± standard error of the mean (SEM). (**B**) Serial 10-fold dilutions of strains containing wild-type *MCM2*, $mcm2_{S164A}$, $mcm2_{S170A}$ or $mcm2_{AA}$ were spotted on YPD plates containing 10, 15 or 20 mM caffeine and grown at 30°C. (**C**) Serial 10-fold dilutions of *MCM2* and $mcm2_{AA}$ were spotted on YPD and YPD containing 10 μg/ml calcofluor white ('CW') before incubation at 30°C.

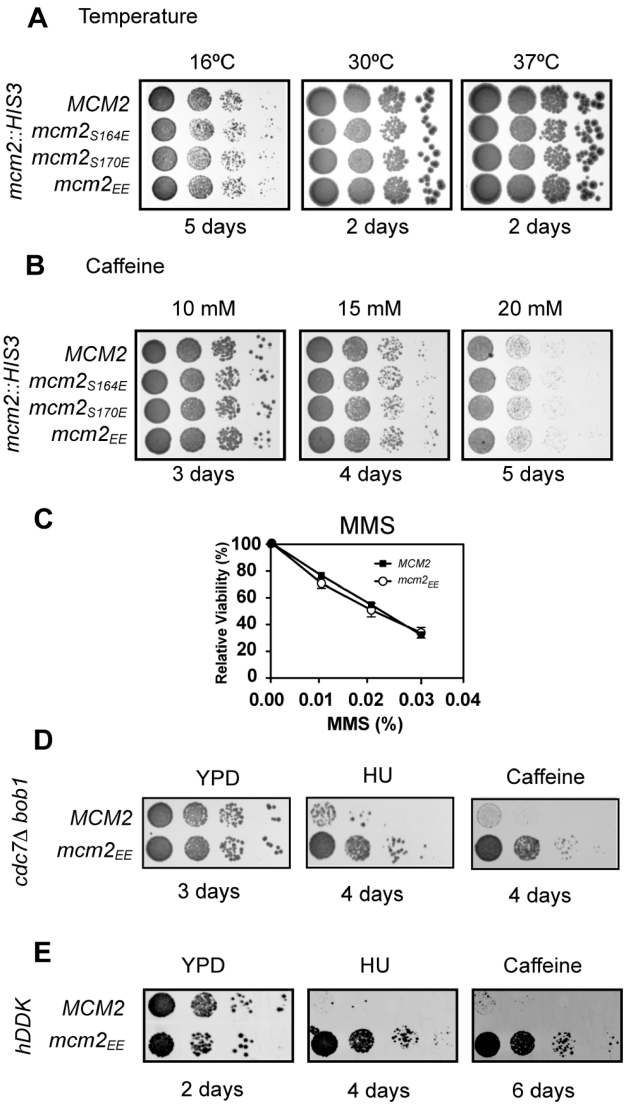


**Figure 3.** Mcm2 phosphomimetic mutants. (**A**) The growth of haploid *mcm2Δ* strains bearing plasmids encoding *MCM2*, $mcm2_{S164E}$, $mcm2_{S170E}$ or $mcm2_{EE}$ was compared. Serial 10-fold dilutions were spotted on YPD plates and grown for 3–5 days at 16, 30 or 37°C. (**B**) Serial 10-fold dilutions of the indicated strains were spotted on YPD media containing 10, 15 or 20 mM caffeine and grown at 30°C. (**C**) The survival of *MCM2* and *mcm2EE*strains after a 4 hour exposure to the indicated concentrations of MMS relative to untreated cells was measured as described (37). (**D**) Ten-fold serial dilutions of haploid *cdc7Δ bob1* strains with wild type *MCM2* or $mcm2_{EE}$ were spotted on YPD with and without HU (100 mM) or caffeine (10 mM) and incubated at 30°C. (**E**) A strain deleted at *cdc7* and *dbf4* and supported for growth with human *CDC7* and *DBF4* was transformed with plasmids encoding *MCM2* or $mcm2_{EE.}$ Ten-fold serial dilutions of the strains were spotted on YPD with or without 150 mM HU or 15 mM caffeine and incubated at 30°C for 2–6 days.

*LEU2* plasmids grew to the same extent as cells containing wild-type *MCM2* on YPD media at all temperatures tested (Figure 3A). Importantly, strains bearing the Glu substitutions at S164 and/or S170 were not sensitive to caffeine, even at the highest concentration of caffeine supplied (20 mM; Figure 3B). $mcm2_{EE}$ cells were also resistant to MMS (Figure 3C). Thus, we concluded that the Glu substitutions at S164 and S170 of Mcm2 were phosphomimetic.

We next addressed whether the putative phosphorylation of S164 and S170 is the result of DDK activity *in vivo*. *CDC7* is essential, but viability of a *cdc7Δ* strain can be restored by the *bob1* mutation in *mcm5* (47). The *cdc7Δ bob1* strain is sensitive to HU (47,48). If Mcm2 is the key target of DDK leading to the HU sensitivity of the *cdc7Δ bob1* strain, then the introduction of $mcm2_{EE}$ should suppress the HU sensitivity. As seen in Figure 3D, $mcm2_{EE}$ does suppresses the HU sensitivity as well as the caffeine sensitivity of the *cdc7Δ bob1* strain. The difference in growth is dependent on the presence of the HU or caffeine since *cdc7Δ bob1* grows similarly on YPD, regardless of whether the *mcm2* allele is wild type or phosphomimic (Figure 3D). This result supports the idea that DDK phosphorylates Mcm2 at S164 and S170; however, it is possible that interaction between *mcm5-bob1* and $mcm2_{EE}$ accounts for the suppression of HU and caffeine sensitivity since *MCM2* and *MCM5* interact genetically (49). A recent study in our lab (Davey,M.J., Andrighetti,H., Ma,X., and Brandl,C.J., manuscript in preparation) has shown that human DDK supports the essential functions of DDK in yeast, but that yeast with human DDK are sensitive to HU and caffeine (Figure 3E). Of particular note, $mcm2_{EE}$ suppresses the sensitivity to HU and caffeine of cells with human DDK (Figure 3E).

The simplest explanation for these observations is that, unlike yeast DDK, human DDK fails to efficiently phosphorylate Mcm2 causing sensitivity to genotoxic agents, and that this defect is rescued by the phosphomimetic nature of $Mcm2_{EE}$. Together, these findings implicate phosphorylation of Mcm2 at S164 and S170 by DDK in response to DNA damage and support the *in vitro* mapping of DDK sites in Mcm2.

### *mcm2$_{AA}$* results in accumulation of Rpa1 foci

In response to treatment with MMS or other replicative stresses, RPA relocalizes from diffuse staining of the nucleus into discrete foci (50,51). Since RPA is a single-stranded DNA (ssDNA)-binding protein, the RPA foci indicate the accumulation of ssDNA. In normal cells responding to DNA damage, ssDNA is likely generated by repair processes (50,52). Using strains containing Rpa1 tagged with green fluorescent protein (GFP), we compared the RPA foci in *mcm2$_{AA}$*, *mcm2$_{EE}$* and wild-type strains before and after exposure to MMS. For comparison we also examined a *mec2-1* strain that is deficient in the S phase checkpoint (53). In untreated *MCM2* cells, GFP-Rpa1 localized to the nucleus with a diffuse signal that transitions into discrete foci after exposure to MMS in 14.9 ± 4.0% of cells (Figure 4). With *mcm2$_{AA}$*, significantly more cells contained foci after MMS treatment (44.3 ± 3.9%), and like the *mec2-1* strain foci were seen without MMS treatment. The *mcm2$_{EE}$* strain had a similar percentage of cells with foci as *MCM2* (11.9 ± 1.0%). These results are consistent with an inability of the *mcm2$_{AA}$* strain to appropriately modulate DNA replication in response to DNA damage.

### Biochemical activities of the phosphomimetic Mcm2-7 complex

To determine mechanisms by which DDK phosphorylation of Mcm2 exerts its control, we examined the effect of phosphorylation of S164 and S170 on Mcm2 activity *in vitro* through use of the phosphomimetic mutations in Mcm2. We reconstituted Mcm2–7 with Mcm2 containing glutamic acid residue substitutions at S164 and S170 ($Mcm2_{EE}$). Note that Mcm proteins are purified from *Escherichia coli* expression strains and thus not phosphorylated. The final step in the reconstitution is a gel filtration column that separates excess free subunits from the complex. Additionally, the gel filtration column allows us to verify that $Mcm2_{WT}$–7 and $Mcm2_{EE}$–7 elute as hexamers (Figure 5A). The peak elution for both complexes occurred around fraction 23, corresponding to a size of ~610 kDa, close to the predicted size of 608 kDa. Analysis of the peak fractions by quantitative western blotting and densitometry of the Coomassie Blue R250-stained gels indicated equal ratios of Mcm2–7 (within ~20%).

We next measured DNA unwinding by $Mcm2_{WT}$–7 and $Mcm2_{EE}$–7 on short oligonucleotide forks whereby DNA unwinding is measured as displacement of a labeled oligonucleotide from its complementary strand. We detected robust unwinding by unphosphorylated $Mcm2_{WT}$–7 (Figure 5B and C). In contrast, DNA unwinding by $Mcm2_{EE}$–7 was reduced to about 40–50% of wild-type

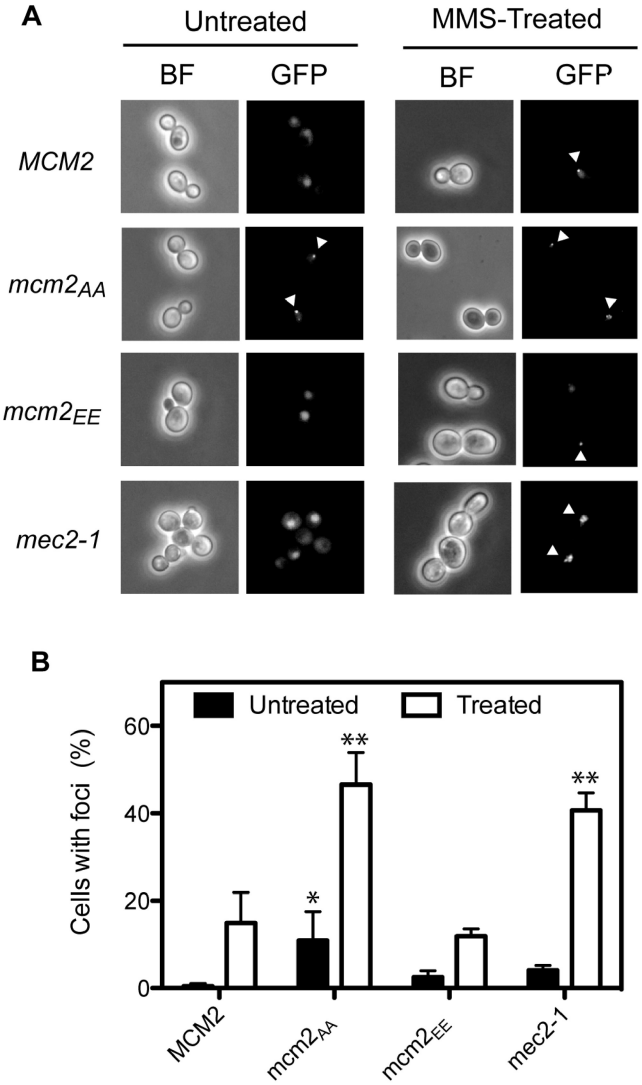


**Figure 4.** Fluorescence microscopy of *MCM2*, *mcm2$_{AA}$* and *mcm2$_{EE}$* cells expressing GFP-tagged Rpa1. (**A**) *MCM2*, *mcm2$_{AA}$*, *mcm2$_{EE}$* and *mec2-1* (53) strains were transformed with a plasmid expressing GFP-Rpa1. Representative bright field ('BF') and fluorescent ('GFP') images of cells from cultures grown at 30°C in YPD or YPD containing 0.03% MMS for 4 h are shown. The white arrowheads indicate foci. Images were taken on a Nikon Ti microscope at 400X. (**B**) The mean percent of cells with RPA foci was calculated by counting >100 cells in three replicate experiments. Strains in which the numbers of cells with RPA foci are significantly different (calculated by ANOVA with Tukey's Multiple Comparison Test) from the *MCM2* strain without MMS ($*P < 0.05$) and with MMS ($**P < 0.05$) are indicated.

levels (Figure 5B and C). This suggests that DDK-dependent modification of Mcm2 at S164 and S170 inhibits DNA unwinding by Mcm2–7. Consistent with this idea, treatment of wild-type Mcm2–7 with DDK and ATP under conditions in which Mcm2 is highly phosphorylated and the principal substrate for DDK (Supplementary Figure S2E and F), also decreased DNA unwinding (Figure 5D).

Models for DNA unwinding by hexameric helicases include binding to single- and/or double-stranded DNA followed by translocation (54–61). Thus, we examined

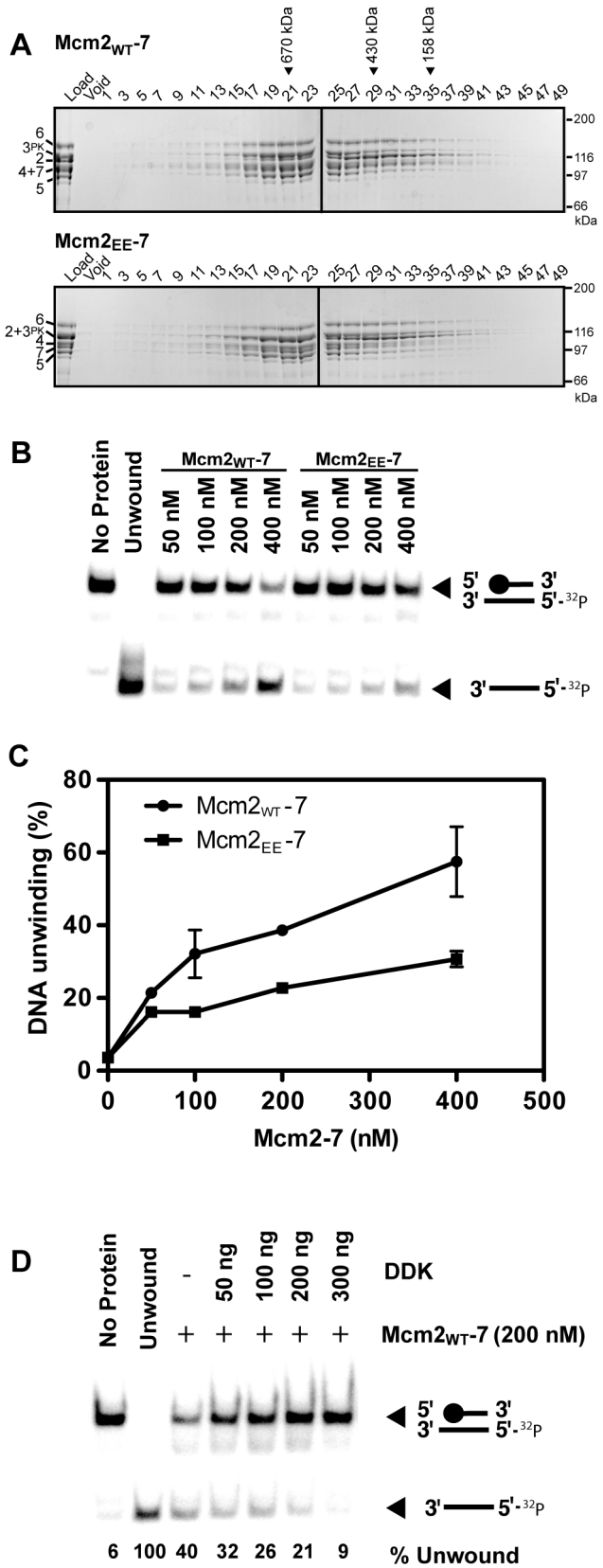


**Figure 5.** Reconstitution of $Mcm2_{WT}$-7 and $Mcm2_{EE}$–7 complexes. (**A**) Mcm2–7 complexes containing wild-type Mcm2 ('$Mcm2_{WT}$–7′) or $Mcm2_{EE}$ ('$Mcm2_{EE}$–7′) were reconstituted from individual subunits. Shown are Coomassie Blue-stained sodium dodecyl sulfate (SDS) polyacrylamide (6%) gels of the fractions from the final gel filtration step. DNA binding by Mcm2–7 containing different versions of Mcm2. We first used a gel filtration-based approach (6), in which binding is measured as the amount of Mcm2–7 that co-elutes with ssDNA. Radiolabeled Mcm2–7 or $Mcm2_{EE}$–7 was incubated with increasing concentrations of M13mp19 circular ssDNA and bound protein separated from free protein via gel filtration. Using this assay we found that $Mcm2_{EE}$–7 binds DNA with higher affinity than Mcm2–7 (Figure 6A). At the lowest concentration of ssDNA supplied (0.5 nM) there was a >3-fold increase of $Mcm2_{EE}$–7 bound to DNA compared to $Mcm2_{WT}$–7. The increased DNA binding with $Mcm2_{EE}$–7 was similar to Mcm2–7 complexes containing ATP site mutations in Mcm2, including $Mcm2_{K549R}$ in which the conserved P-loop lysine is replaced with an arginine residue [Figure 6A and (6)]. These initial experiments indicated that Mcm2–7 complexes containing $Mcm2_{EE}$ or $Mcm2_{K549R}$ have higher affinity for ssDNA than complexes containing wild-type Mcm2. To confirm that $Mcm2_{EE}$ mimics the effects of phosphorylation, we treated $Mcm2_{WT}$–7 with DDK and ATP before measuring DNA binding. An increase of ~2.5–5-fold was observed when Mcm2–7 was phosphorylated by DDK compared to mock-treated (no DDK) Mcm2–7 (Figure 6B).

DNA binding was also measured by EMSAs, which allow a wider range of concentrations. Increasing amounts of $Mcm2_{WT}$–7, $Mcm2_{EE}$–7 or $Mcm2_{K549R}$–7 were incubated with 1 nM poly-$dT_{60}$. Binding of Mcm2–7 shifted the DNA to a point near the top of the gel that coincided with the migration of Mcm2–7 as visualized by staining (Figure 6C and D) or western blotting (data not shown). $Mcm2_{WT}$–7 shifted up to 30 fmol of the ssDNA supplied. This binding is similar to previous reports using this approach (62) and approximates the affinity observed by gel filtration. In contrast, $Mcm2_{EE}$–7 shifted 8- to 10-fold more poly-$dT_{60}$ (Figure 6C and D). $Mcm2_{K549R}$–7 shifted even more ssDNA at levels 15- to 18-fold over Mcm2-7 (Figure 6C and D). Overall, these results demonstrate that the phosphomimetic mutations in Mcm2 enhance ssDNA binding by Mcm2–7.

At first glance, our data seem contradictory. Mcm2–7 containing the $Mcm2_{EE}$ mutant binds DNA better than wild type, but unwinds DNA less well, an activity that requires DNA binding. However, we reasoned that $Mcm2_{EE}$–7 may bind DNA too tightly, impairing the ability of Mcm2–7 to translocate along DNA. To test this, we examined whether adding NaCl to the

**Figure 5.** Continued
The elution of molecular size standards from the column is indicated above the gels. The migration of molecular size markers and of Mcms through the gels is indicated on the left and right, respectively. (**B**) DNA unwinding by $Mcm2_{WT}$–7 and $Mcm2_{EE}$–7 on synthetic fork substrates was examined. The peak fraction from each reconstitution was assayed for DNA unwinding. 'Unwound' is a control that indicates the extent of reannealing of unwound substrate. The migrations of double-stranded substrate and single-stranded product are indicated on the right. (**C**) The mean extent of DNA unwinding ± SEM by the indicated amount of each complex was calculated from three replicate experiments. (**D**) DNA unwinding by $Mcm2_{WT}$–7 (200 nM) after treatment with DDK is shown. The extent of unwinding is indicated below the gel.

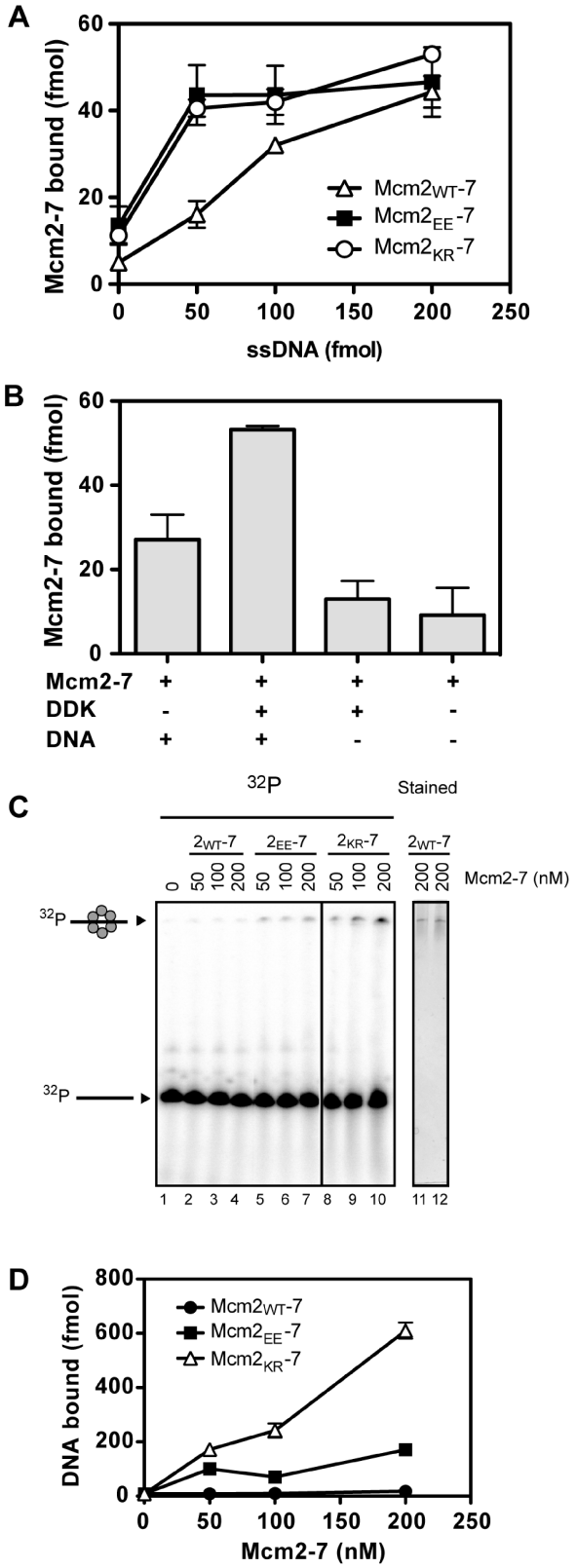


**Figure 6.** ssDNA binding by Mcm2–7. (**A**) DNA binding was measured using a gel filtration-based assay (6). Binding of $Mcm2_{WT}$–7 (open triangle), $Mcm2_{EE}$–7 (filled square) and $Mcm2_{KR}$–7 (open circle) was determined in triplicate experiments and the mean plotted. Representative elution profiles for each point are shown in Supplementary Figure S3. (**B**) Mcm2–7 (200 fmol) was incubated in assay buffer with 100 μM ATP with or without DDK for 30 min at 30°C before addition of 50 fmol ssDNA and ATP to 5 mM. After incubation for 10 min at 37°C, the samples were analyzed by gel filtration. The mean amount of Mcm2–7 that co-eluted with DNA in triplicate experiments was determined. (**C**) A Phosphor screen image of a representative EMSA. The migration of free DNA and protein–DNA complex is indicated on the left. A portion of a gel containing free protein and protein–DNA complex was removed and stained with GelCode Blue (Pierce) and is shown on the right. (**D**) The mean amount of DNA shifted was calculated and plotted with SEM from three replicate experiments.

DNA-binding assay would reduce the $Mcm2_{EE}$–7–DNA interaction. Indeed, when NaCl was present at 100 mM, $Mcm2_{EE}$–7 binding to DNA decreased to a level observed with $Mcm2_{WT}$–7 (Figure 7A). Moreover, when NaCl was added to $Mcm2_{EE}$–7 in a DNA-unwinding assay, the amount of unwound substrate increased to a level comparable to $Mcm2_{WT}$–7 (Figure 7B). These observations suggested that the defect in DNA unwinding by $Mcm2_{EE}$–7 results from enhanced DNA binding.

Since the *mcm2*$_{K549R}$ mutation decreases ATP hydrolysis by Mcm2 (6) and like $Mcm2_{EE}$ increases binding to ssDNA by Mcm2–7, we examined whether phosphorylation of Mcm2 affects ATP hydrolysis by Mcm2. The ATP sites of Mcm2–7 are found at subunit interfaces and residues from two subunits are required to form a functional ATP site [Figure 8A; (3,4)]. Accordingly, ATP hydrolysis by Mcm2 is dependent on Mcm6 (3,4). The Mcm2/6 ATP site makes only a small contribution to the total ATP hydrolysis by Mcm2–7 (2) and even a large change in Mcm2 activity has only a modest effect on the intact complex. Thus, we initially measured ATP hydrolysis by the Mcm2/6 pair rather than the intact Mcm2–7 complex. Wild-type, unphosphorylated Mcm2 with Mcm6 hydrolyzed ATP at a rate of $4.9 \pm 0.1\,min^{-1}$ (Figure 8B). When $Mcm2_{EE}$ was mixed with Mcm6, ATP hydrolysis was reduced to ~75% of wild-type Mcm2/6 ($3.6 \pm 0.6\,min^{-1}$). For comparison, ATP hydrolysis by $Mcm2_{K549R}$ was $0.9 \pm 0.0\,min^{-1}$. $Mcm2_{AA}$ had activity similar to wild-type Mcm2 ($4.7 \pm 0.1\,min^{-1}$) as would be expected since the proteins are purified from *E. coli* and hence not phosphorylated (Figure 8B). We also measured the effects of the $Mcm2_{EE}$ mutation on the ATPase activity of the intact complex. There was no significant difference in the rates of $Mcm2_{EE}$–7 ($18.0 \pm 0.2\,min^{-1}$, $P > 0.05$, $n = 3$) and $Mcm2_{WT}$–7 ($21.0 \pm 1.6\,min^{-1}$; Figure 8C). For comparison, we also show ATP hydrolysis by $Mcm2_{KR}$–7 ($17.4 \pm 0.4\,min^{-1}$; Figure 8C). The lack of significant difference is not surprising considering the small contribution of Mcm2/6 to the ATPase of intact Mcm2–7.

## Mcm2 phosphorylation affects Mcm2–7 activity *in vivo*

As shown in Figure 8D, cells bearing *mcm2*$_{K549R}$ are sensitive to caffeine similar to *mcm2*$_{AA}$ even though some of the biochemical properties of $Mcm2_{K549R}$ are more similar to $Mcm2_{EE}$, which does not lead to caffeine sensitivity. To examine the relationship between the changes observed *in vitro* and the sensitivity to caffeine, we made *mcm2* alleles mutated at both the ATP site (K549R) and the

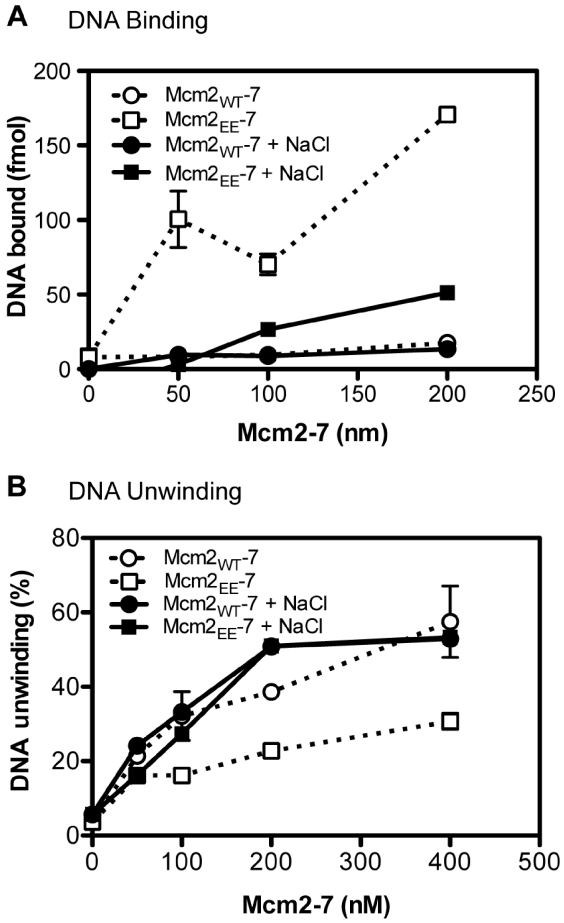


**Figure 7.** Disruption of DNA binding rescues the DNA unwinding defect of $Mcm2_{EE}$–7. (**A**) DNA binding by the indicated concentrations of $Mcm2_{WT}$–7 (black circle) and $Mcm2_{EE}$–7 (black square) in the presence of 100 mM NaCl was measured by EMSA and plotted. DNA binding by $Mcm2_{WT}$–7 (white circle) and $Mcm2_{EE}$–7 (white square) in the absence of NaCl is shown for comparison. (**B**) DNA unwinding by the indicated concentrations of $Mcm2_{WT}$–7 (black circle) and $Mcm2_{EE}$–7 (black square) in the presence of 100 mM NaCl was measured. DNA unwinding by $Mcm2_{WT}$–7 (white circle) and $Mcm2_{EE}$–7 (white square) in the absence of NaCl is shown for comparison.

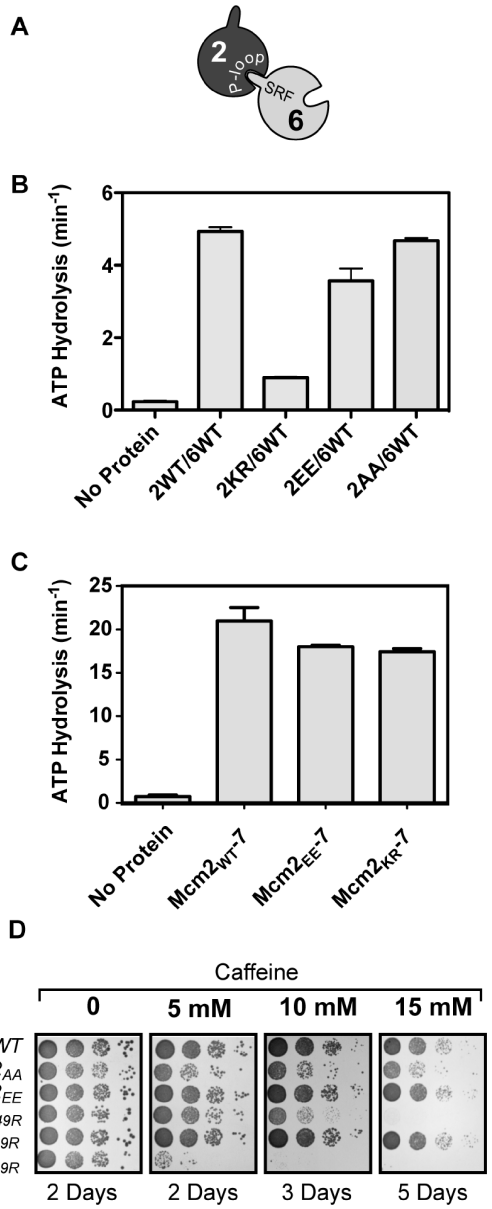


**Figure 8.** Phosphomimetic mutations in Mcm2 reduce ATP hydrolysis. (**A**) A schematic showing the Mcm2/6 subunit interface. The phosphate binding loop (P-loop) of Mcm2 and the SRF motif of Mcm6, required for ATP hydrolysis by Mcm2 are indicated. K549 is located in the P-loop. (**B**) ATP hydrolysis by recombinantly expressed Mcm2, $Mcm2_{EE}$, $Mcm2_{AA}$ and $Mcm2_{K549R}$ in the presence of Mcm6 was measured. The rate of ATP hydrolysis by each pair was calculated and plotted with the standard error of the mean. The rate of hydrolysis by each complex, except between Mcm2/6 and $Mcm2_{AA}$/6, is significantly different ($P < 0.01$; $n = 3$). (**C**) ATP hydrolysis by Mcm2–7, $Mcm2_{EE}$–7 and $Mcm2_{KR}$–7 was measured in triplicate at 1 mM ATP, the rate calculated and plotted with SEM. (**D**) Haploid strains deleted at *mcm2* and containing plasmid-encoded wild-type *MCM2*, $mcm2_{AA}$, $mcm2_{EE}$, $mcm2_{AA,K549R}$ or $mcm2_{EE,K549R}$ were serially diluted 10-fold and then spotted on YPD with the indicated concentrations of caffeine and grown at 30°C.

DDK phosphorylation sites (EE or AA). Cells containing $mcm2_{K549R,EE}$ and $mcm2_{K549R,AA}$ as the sole copy of *mcm2* grew similarly to wild-type cells on YPD (Figure 8D). Interestingly, when spotted onto YPD containing caffeine, the growth of the $mcm2_{K549R,EE}$ strain was markedly reduced relative to both wild-type cells and cells containing the individual mutations (Figure 8D). In contrast, strains with a non-phosphorylatable Mcm2 containing the ATP site mutation ($mcm2_{K549R,\ AA}$) were not sensitive to caffeine. These results suggest that a precise range of Mcm2–7 activity is required for cells to respond to DNA damage.

## DISCUSSION

### Phosphorylation of Mcm2 and cell viability

Here, we show that *S. cerevisiae* containing Mcm2 that lacks the phosphorylation sites, S164 and/or S170, are viable and progress normally through S phase when Mcm2 is expressed at endogenous levels. Our results are consistent with the recent finding that normal growth is unaffected by deletion of the N-terminal region of Mcm2

(12) or mutation of several phosphorylation sites to alanine (11). Furthermore, it has been demonstrated that phosphorylation of Mcm4 by DDK is sufficient for replication in budding yeast (11,12). These results contrast with the finding that $Mcm2_{S170A}$ expressed from the *GAL10* promoter did not support viability (21). We have replicated this latter result, indicating that the cellular effect of $Mcm2_{S170A}$ is concentration dependent (Supplementary Figure S4). It may be that overexpression of Mcm2 causes genomic instability that is dealt with in normally functioning cells, but requires phosphorylation of Mcm2 at S170.

### Phosphorylation of Mcm2 *in vivo*

We propose that phosphorylation of Mcm2 at S164 and S170 is important in response to DNA damage. The sensitivity of the $mcm2_{AA}$ strain to caffeine and MMS, the accumulation of RPA foci in this strain and the reversal of these phenotypes by $mcm2_{EE}$ strongly suggest a role in the response to DNA damage. MMS is a well-defined base alkylating agent that induces specific cellular responses including S phase checkpoint (63). Caffeine is a purine analog that inhibits kinases of the PI3K-like family, which include the checkpoint kinases, Tel1 and Mec1 (43,45). Inhibition of the checkpoint kinases by caffeine can lead to accumulation of DNA damage (42). Thus, the caffeine sensitive phenotype of cells with $mcm2_{AA}$ may not occur in response to inhibition of PI3K-like kinases *per se* but rather in response to DNA damage generated by high doses of caffeine.

We have mapped S164 and S170 *in vitro* as potential DDK sites, consistent with a previous study (21). Two lines of evidence support the idea that these are DDK phosphorylation sites *in vivo*. First, $mcm2_{EE}$ suppresses the HU and caffeine sensitivity of a *cdc7Δ bob1* strain. Second, the HU and caffeine sensitivity of a strain containing human DDK is also suppressed by $mcm2_{EE}$. Furthermore, Mcm2 is already known to be a substrate for DDK in yeast (17) and DDK is known to have roles in responding to DNA damage (26,34,38,40,41,64)

We note that a recent study from the Bell lab indicates that at least a portion of Mcm2 is phosphorylated at S164 and S170 in a CK2-dependent manner in G1 arrested cells (11). Interestingly, DDK and CK2 share similar specificity, targeting acidic sites (65,66). Our work strongly implicates DDK as the kinase that phosphorylates Mcm2 in the response to DNA damage; however, we cannot eliminate the possibility that CK2 has a role. In yeast, the regulatory subunits of CK2 (Ckb1 and Ckb2) are required for recovery from checkpoint and adaptation to promote interaction between a phosphatase (Ptc2) and the checkpoint kinase, Rad53 (67).

### Regulation of Mcm2–7 activities by phosphorylation of Mcm2

We propose that phosphorylation of Mcm2 at S164 and/or S170 controls Mcm2-7 *in vivo* by altering its DNA binding and/or helicase activities. Phosphorylation at S164 and S170 of Mcm2, which increases DNA binding by Mcm2-7 *in vitro*, may stabilize binding of Mcm2-7 to chromatin when cells respond to DNA damage. Mcm2–7 is more abundant on chromatin than is expected for one complex at each replication fork (1). In mammalian and *Xenopus* cells, the 'excess' Mcm2–7 is not required for normal cell growth but is important when cells are placed under replicative stress (68–70). Alternatively, the decreased DNA unwinding elicited by phosphorylation of Mcm2 may be required in response to DNA damage to slow replication forks and allow time for repair of damaged DNA.

It is possible that the effects on DNA binding and unwinding are mediated through the Mcm2 ATP site since the ATP hydrolysis by the Mcm2/6 site is decreased with the phosphomimetic mutation in Mcm2. Consistent with this idea, the effect of $Mcm2_{EE}$ on DNA binding by Mcm2–7 is similar to what is observed for a mutation that affects ATP hydrolysis by the Mcm2/6 site, $Mcm2_{K549R}$. Additional studies will be required to determine the exact relationship between ATP hydrolysis by Mcm2/6 and the different phenotypes of *MCM2*, $mcm2_{AA}$, $mcm2_{EE}$ and $mcm2_{K549R}$. In this regard, we cannot exclude that it is the differences in DNA unwinding or an as yet unexamined activity of Mcm2-7 that accounts for the different phenotypes.

Regardless of which activity results in the caffeine sensitivity, relatively small changes detected *in vitro* result in significant changes in sensitivity to caffeine *in vivo*. This level of sensitivity to modest changes detected *in vitro* is not without precedence. An ATP site mutation in the P1 plasmid partition protein, ParA, results in a decrease to about 1/3 of wild-type activity, but has a >20-fold effect on the autorepressor activity of ParA *in vivo* (71).

## SUPPLEMENTARY DATA

Supplementary Data are available at NAR online.

## ACKNOWLEDGEMENTS

The authors are grateful to Dave Edgell for his comments on the manuscript and to Xiaoli Ma for expert technical assistance. We also thank Heather Andrighetti for construction of the yeast strain with human DDK and Bernard Duncker for the *mec2-1* strain.

## FUNDING

The Canadian Institutes of Health Research (MOP 68926 to M.J.D.); a Natural Science and Engineering Research Council Doctoral Award and Schulich Graduate Awards (to B.E.S.). M.J.D. is a Research Scientist of the Canadian Cancer Society Research Institute. Funding for open access charge: Canadian Institutes of Health Research/University of Western Ontario.

*Conflict of interest statement*. None declared.

## REFERENCES


1. Forsburg,S.L. (2004) Eukaryotic MCM proteins: beyond replication initiation. *Microbiol. Mol. Biol. Rev.*, **68**, 109–131.
2. Bochman,M.L., Bell,S.P. and Schwacha,A. (2008) Subunit organization of Mcm2-7 and the unequal role of active sites in ATP hydrolysis and viability. *Mol. Cell. Biol.*, **28**, 5865–5873.
3. Davey,M.J., Indiani,C. and O'Donnell,M. (2003) Reconstitution of the Mcm2-7p heterohexamer, subunit arrangement, and ATP site architecture. *J. Biol. Chem.*, **278**, 4491–4499.
4. Schwacha,A. and Bell,S.P. (2001) Interactions between two catalytically distinct MCM subgroups are essential for coordinated ATP hydrolysis and DNA replication. *Mol. Cell*, **8**, 1093–1104.
5. Bochman,M.L. and Schwacha,A. (2008) The Mcm2-7 Complex has *in vitro* helicase activity. *Mol. Cell*, **31**, 287–293.
6. Stead,B.E., Sorbara,C.D., Brandl,C.J. and Davey,M.J. (2009) ATP binding and hydrolysis by Mcm2 regulate DNA binding by Mcm complexes. *J. Mol. Biol.*, **391**, 301–313.
7. Ishimi,Y. and Komamura-Kohno,Y. (2001) Phosphorylation of Mcm4 at specific sites by cyclin-dependent kinase leads to loss of Mcm4,6,7 helicase activity. *J. Biol. Chem.*, **276**, 34428–34433.
8. Liku,M.E., Nguyen,V.Q., Rosales,A.W., Irie,K. and Li,J.J. (2005) CDK phosphorylation of a novel NLS-NES module distributed between two subunits of the Mcm2-7 complex prevents chromosomal rereplication. *Mol. Biol. Cell*, **16**, 5026–5039.
9. Yoo,H.Y., Shevchenko,A. and Dunphy,W.G. (2004) Mcm2 is a direct substrate of ATM and ATR during DNA damage and DNA replication checkpoint responses. *J. Biol. Chem.*, **279**, 53353–53364.
10. Cortez,D., Glick,G. and Elledge,S.J. (2004) Minichromosome maintenance proteins are direct targets of the ATM and ATR checkpoint kinases. *Proc. Natl Acad. Sci. USA*, **101**, 10078–10083.
11. Randell,J.C.W., Fan,A., Chan,C., Francis,L.I., Heller,R.C., Galani,K. and Bell,S.P. (2010) Mec1 is one of multiple kinases that prime the Mcm2-7 helicase for phosphorylation by Cdc7. *Mol. Cell*, **40**, 353–363.
12. Sheu,Y.J. and Stillman,B. (2010) The Dbf4-Cdc7 kinase promotes S phase by alleviating an inhibitory activity in Mcm4. *Nature*, **463**, 113–117.
13. Sheu,Y.J. and Stillman,B. (2006) Cdc7-Dbf4 phosphorylates MCM proteins via a docking site-mediated mechanism to promote S phase progression. *Mol. Cell*, **24**, 101–113.
14. Zou,L. and Stillman,B. (2000) Assembly of a complex containing Cdc45p, replication protein A, and Mcm2p at replication origins controlled by S-phase cyclin-dependent kinases and Cdc7p-Dbf4p kinase. *Mol. Cell. Biol.*, **20**, 3086–3096.
15. Bousset,K. and Diffley,J.F. (1998) The Cdc7 protein kinase is required for origin firing during S phase. *Genes Dev.*, **12**, 480–490.
16. Sato,N., Arai,K. and Masai,H. (1997) Human and *Xenopus* cDNAs encoding budding yeast Cdc7-related kinases: in vitro phosphorylation of MCM subunits by a putative human homologue of Cdc7. *EMBO J.*, **16**, 4340–4351.
17. Lei,M., Kawasaki,Y., Young,M.R., Kihara,M., Sugino,A. and Tye,B.K. (1997) Mcm2 is a target of regulation by Cdc7-Dbf4 during the initiation of DNA synthesis. *Genes Dev.*, **11**, 3365–3374.
18. Brown,G.W. and Kelly,T.J. (1998) Purification of Hsk1, a minichromosome maintenance protein kinase from fission yeast. *J. Biol. Chem.*, **273**, 22083–22090.
19. Snaith,H.A., Brown,G.W. and Forsburg,S.L. (2000) *Schizosaccharomyces pombe* Hsk1p is a potential cds1p target required for genome integrity. *Mol. Cell. Biol.*, **20**, 7922–7932.
20. Francis,L.I., Randell,J.C., Takara,T.J., Uchima,L. and Bell,S.P. (2009) Incorporation into the prereplicative complex activates the Mcm2-7 helicase for Cdc7-Dbf4 phosphorylation. *Genes Dev.*, **23**, 643–654.
21. Bruck,I. and Kaplan,D. (2009) Dbf4-Cdc7 phosphorylation of Mcm2 is required for cell growth. *J. Biol. Chem.*, **284**, 28823–28831.
22. Montagnoli,A., Valsasina,B., Brotherton,D., Troiani,S., Rainoldi,S., Tenca,P., Molinari,A. and Santocanale,C. (2006) Identification of Mcm2 phosphorylation sites by S-phase-regulating kinases. *J. Biol. Chem.*, **281**, 10281–10290.
23. Masai,H., Taniyama,C., Ogino,K., Matsui,E., Kakusho,N., Matsumoto,S., Kim,J.M., Ishii,A., Tanaka,T., Kobayashi,T. *et al.* (2006) Phosphorylation of MCM4 by Cdc7 kinase facilitates its interaction with Cdc45 on the chromatin. *J. Biol. Chem.*, **281**, 39249–39261.
24. Cho,W.H., Lee,Y.J., Kong,S.I., Hurwitz,J. and Lee,J.K. (2006) CDC7 kinase phosphorylates serine residues adjacent to acidic amino acids in the minichromosome maintenance 2 protein. *Proc. Natl Acad. Sci. USA*, **103**, 11521–11526.
25. Tsuji,T., Ficarro,S.B. and Jiang,W. (2006) Essential role of phosphorylation of MCM2 by Cdc7/Dbf4 in the initiation of DNA replication in mammalian cells. *Mol. Biol. Cell*, **17**, 4459–4472.
26. Weinreich,M. and Stillman,B. (1999) Cdc7p-Dbf4p kinase binds to chromatin during S phase and is regulated by both the APC and the RAD53 checkpoint pathway. *EMBO J.*, **18**, 5334–5346.
27. Ke,S.H. and Madison,E.L. (1997) Rapid and efficient site-directed mutagenesis by single-tube 'megaprimer' PCR method. *Nucleic Acids Res.*, **25**, 3371–3372.
28. Gietz,R.D. and Sugino,A. (1988) New yeast-*Escherichia coli* shuttle vectors constructed with in vitro mutagenized yeast genes lacking six-base pair restriction sites. *Gene*, **74**, 527–534.
29. Hoke,S.M., Guzzo,J., Andrews,B. and Brandl,C.J. (2008) Systematic genetic array analysis links the *Saccharomyces cerevisiae* SAGA/SLIK and NuA4 component Tra1 to multiple cellular processes. *BMC Genet.*, **9**, 46.
30. Scherer,S. and Davis,R.W. (1979) Replacement of chromosome segments with altered DNA sequences constructed in vitro. *Proc. Natl Acad. Sci. USA*, **76**, 4951–4955.
31. Brachmann,C.B., Davies,A., Cost,G.J., Caputo,E., Li,J., Hieter,P. and Boeke,J.D. (1998) Designer deletion strains derived from *Saccharomyces cerevisiae* S288C: a useful set of strains and plasmids for PCR-mediated gene disruption and other applications. *Yeast*, **14**, 115–132.
32. Pan,X., Yuan,D.S., Xiang,D., Wang,X., Sookhai-Mahadeo,S., Bader,J.S., Hieter,P., Spencer,F. and Boeke,J.D. (2004) A robust toolkit for functional profiling of the yeast genome. *Mol. Cell*, **16**, 487–496.
33. Costanzo,V., Shechter,D., Lupardus,P.J., Cimprich,K.A., Gottesman,M. and Gautier,J. (2003) An ATR- and Cdc7-dependent DNA damage checkpoint that inhibits initiation of DNA replication. *Mol. Cell*, **11**, 203–213.
34. Duncker,B.P. and Brown,G.W. (2003) Cdc7 kinases (DDKs) and checkpoint responses: lessons from two yeasts. *Mutat. Res.*, **532**, 21–27.
35. Ogi,H., Wang,C.Z., Nakai,W., Kawasaki,Y. and Masumoto,H. (2008) The role of the *Saccharomyces cerevisiae* Cdc7-Dbf4 complex in the replication checkpoint. *Gene*, **414**, 32–40.
36. Tsuji,T., Lau,E., Chiang,G.G. and Jiang,W. (2008) The role of Dbf4/Drf1-dependent kinase Cdc7 in DNA-damage checkpoint control. *Mol. Cell*, **32**, 862–869.
37. Varrin,A.E., Prasad,A.A., Scholz,R.P., Ramer,M.D. and Duncker,B.P. (2005) A mutation in Dbf4 motif M impairs interactions with DNA replication factors and confers increased resistance to genotoxic agents. *Mol. Cell. Biol.*, **25**, 7494–7504.
38. Fung,A.D., Ou,J., Bueler,S. and Brown,G.W. (2002) A conserved domain of *Schizosaccharomyces pombe* dfp1+ is uniquely required for chromosome stability following alkylation damage during S phase. *Mol. Cell. Biol.*, **22**, 4477–4490.
39. Jares,P., Donaldson,A. and Blow,J.J. (2000) The Cdc7/Dbf4 protein kinase: target of the S phase checkpoint? *EMBO Rep.*, **1**, 319–322.
40. Gabrielse,C., Miller,C.T., McConnell,K.H., DeWard,A., Fox,C.A. and Weinreich,M. (2006) A Dbf4p BRCA1 C-terminal-like domain required for the response to replication fork arrest in budding yeast. *Genetics*, **173**, 541–555.
41. Jones,D.R., Prasad,A.A., Chan,P.K. and Duncker,B.P. (2010) The Dbf4 motif C zinc finger promotes DNA replication and mediates resistance to genotoxic stress. *Cell Cycle*, **9**, 2018–2026.
42. Kuranda,K., Leberre,V., Sokol,S., Palamarczyk,G. and Francois,J. (2006) Investigating the caffeine effects in the yeast *Saccharomyces cerevisiae* brings new insights into the connection

between TOR, PKC and Ras/cAMP signalling pathways. *Mol. Microbiol.*, **61**, 1147–1166.
43. Moser,B.A., Brondello,J.M., Baber-Furnari,B. and Russell,P. (2000) Mechanism of caffeine-induced checkpoint override in fission yeast. *Mol. Cell. Biol.*, **20**, 4288–4294.
44. Reinke,A., Chen,J.C., Aronova,S. and Powers,T. (2006) Caffeine targets TOR complex I and provides evidence for a regulatory link between the FRB and kinase domains of Tor1p. *J. Biol. Chem.*, **281**, 31616–31626.
45. Saiardi,A., Resnick,A.C., Snowman,A.M., Wendland,B. and Snyder,S.H. (2005) Inositol pyrophosphates regulate cell death and telomere length through phosphoinositide 3-kinase-related protein kinases. *Proc. Natl Acad. Sci. USA*, **102**, 1911–1914.
46. Levin,D.E. (2005) Cell wall integrity signaling in *Saccharomyces cerevisiae*. *Microbiol. Mol. Biol. Rev.*, **69**, 262–291.
47. Hardy,C.F., Dryga,O., Seematter,S., Pahl,P.M. and Sclafani,R.A. (1997) mcm5/cdc46-bob1 bypasses the requirement for the S phase activator Cdc7p. *Proc. Natl Acad. Sci. USA*, **94**, 3151–3155.
48. Dohrmann,P.R., Oshiro,G., Tecklenburg,M. and Sclafani,R.A. (1999) RAD53 regulates DBF4 independently of checkpoint function in *Saccharomyces cerevisiae*. *Genetics*, **151**, 965–977.
49. Bochman,M.L. and Schwacha,A. (2010) The *Saccharomyces cerevisiae* Mcm6/2 and Mcm5/3 ATPase active sites contribute to the function of the putative Mcm2-7 'gate'. *Nucleic Acids Res.*, **38**, 6078–6088.
50. Bernstein,K.A., Shor,E., Sunjevaric,I., Fumasoni,M., Burgess,R.C., Foiani,M., Branzei,D. and Rothstein,R. (2009) Sgs1 function in the repair of DNA replication intermediates is separable from its role in homologous recombinational repair. *EMBO J.*, **28**, 915–925.
51. Wu,X., Shell,S.M. and Zou,Y. (2005) Interaction and colocalization of Rad9/Rad1/Hus1 checkpoint complex with replication protein A in human cells. *Oncogene*, **24**, 4728–4735.
52. Clausing,E., Mayer,A., Chanarat,S., Muller,B., Germann,S.M., Cramer,P., Lisby,M. and Strasser,K. (2010) The transcription elongation factor Bur1-Bur2 interacts with replication protein A and maintains genome stability during replication stress. *J. Biol. Chem.*, **285**, 41665–41674.
53. Weinert,T.A., Kiser,G.L. and Hartwell,L.H. (1994) Mitotic checkpoint genes in budding yeast and the dependence of mitosis on DNA replication and repair. *Genes Dev.*, **8**, 652–665.
54. Liu,W., Pucci,B., Rossi,M., Pisani,F.M. and Ladenstein,R. (2008) Structural analysis of the *Sulfolobus solfataricus* MCM protein N-terminal domain. *Nucleic Acids Res.*, **36**, 3235–3243.
55. Kaplan,D.L., Davey,M.J. and O'Donnell,M. (2003) Mcm4,6,7 uses a "pump in ring" mechanism to unwind DNA by steric exclusion and actively translocate along a duplex. *J. Biol. Chem.*, **278**, 49171–49182.
56. Kelman,Z. and Hurwitz,J. (2003) Structural lessons in DNA replication from the third domain of life. *Nat. Struct. Biol.*, **10**, 148–150.
57. Lee,J.K. and Hurwitz,J. (2001) Processive DNA helicase activity of the minichromosome maintenance proteins 4, 6, and 7 complex requires forked DNA structures. *Proc Natl Acad Sci USA*, **98**, 54–59.
58. Sato,M., Gotow,T., You,Z., Komamura-Kohno,Y., Uchiyama,Y., Yabuta,N., Nojima,H. and Ishimi,Y. (2000) Electron microscopic observation and single-stranded DNA binding activity of the Mcm4,6,7 complex. *J. Mol. Biol.*, **300**, 421–431.
59. VanLoock,M.S., Alexandrov,A., Yu,X., Cozzarelli,N.R. and Egelman,E.H. (2002) SV40 large T antigen hexamer structure: domain organization and DNA-induced conformational changes. *Curr. Biol.*, **12**, 472–476.
60. Hacker,K.J. and Johnson,K.A. (1997) A hexameric helicase encircles one DNA strand and excludes the other during DNA unwinding. *Biochemistry*, **36**, 14080–14087.
61. Egelman,E.H., Yu,X., Wild,R., Hingorani,M.M. and Patel,S.S. (1995) Bacteriophage T7 helicase/primase proteins form rings around single-stranded DNA that suggest a general structure for hexameric helicases. *Proc. Natl Acad. Sci. USA*, **92**, 3869–3873.
62. Bochman,M.L. and Schwacha,A. (2007) Differences in the single-stranded DNA binding activities of MCM2-7 and MCM467: MCM2 and MCM5 define a slow ATP-dependent step. *J. Biol. Chem.*, **282**, 33795–33804.
63. Beranek,D.T. (1990) Distribution of methyl and ethyl adducts following alkylation with monofunctional alkylating agents. *Mutat. Res.*, **231**, 11–30.
64. Pessoa-Brandao,L. and Sclafani,R.A. (2004) CDC7/DBF4 functions in the translesion synthesis branch of the RAD6 epistasis group in *Saccharomyces cerevisiae*. *Genetics*, **167**, 1597–1610.
65. Songyang,Z., Lu,K., Kwon,Y., Tsai,L., Filhol,O., Cochet,C., Brickey,D., Soderling,T., Bartleson,C., Graves,D. *et al.* (1996) A structural basis for substrate specificities of protein Ser/Thr kinases: primary sequence preference of casein kinases I and II, NIMA, phosphorylase kinase, calmodulin-dependent kinase II, CDK5, and Erk1. *Mol. Cell. Biol.*, **16**, 6486–6493.
66. Mok,J., Kim,P.M., Lam,H.Y., Piccirillo,S., Zhou,X., Jeschke,G.R., Sheridan,D.L., Parker,S.A., Desai,V., Jwa,M. *et al.* (2010) Deciphering protein kinase specificity through large-scale analysis of yeast phosphorylation site motifs. *Sci. Signal*, **3**, ra12.
67. Guillemain,G., Ma,E., Mauger,S., Miron,S., Thai,R., Guerois,R., Ochsenbein,F. and Marsolier-Kergoat,M.-C. (2007) Mechanisms of checkpoint kinase Rad53 inactivation after a double-strand break in *Saccharomyces cerevisiae*. *Mol. Cell. Biol.*, **27**, 3378–3389.
68. Ge,X.Q., Jackson,D.A. and Blow,J.J. (2007) Dormant origins licensed by excess Mcm2-7 are required for human cells to survive replicative stress. *Genes Dev.*, **21**, 3331–3341.
69. Ibarra,A., Schwob,E. and Mendez,J. (2008) Excess MCM proteins protect human cells from replicative stress by licensing backup origins of replication. *Proc. Natl Acad. Sci. USA*, **105**, 8956–8961.
70. Woodward,A.M., Gohler,T., Luciani,M.G., Oehlmann,M., Ge,X., Gartner,A., Jackson,D.A. and Blow,J.J. (2006) Excess Mcm2-7 license dormant origins of replication that can be used under conditions of replicative stress. *J. Cell Biol.*, **173**, 673–683.
71. Fung,E., Bouet,J.Y. and Funnell,B.E. (2001) Probing the ATP-binding site of P1 ParA: partition and repression have different requirements for ATP binding and hydrolysis. *EMBO J.*, **20**, 4901–4911.